Lawrence Berkeley National Laboratory
Recent Work

Title
REACTIVE AND INELASTIC SCATTERING OF H2 + D2 USING A REPULSIVE MODEL POTENTIAL ENERGY SURFACE

Permalink
https://escholarship.org/uc/item/6m2742sq

Author
Brown, N.J.

Publication Date
1978-04-01

eScholarship.org Powered by the California Digital Library
University of California

LBL-9539
Preprint

Lawrence Berkeley Laboratory
UNIVERSITY OF CALIFORNIA

ENERGY & ENVIRONMENT
DIVISION

Submitted to the Journal of Chemical Physics

REACTIVE AND INELASTIC SCATTERING OF H_2 + D_2 USING A REPULSIVE MODEL POTENTIAL ENERGY SURFACE

Nancy J. Brown and David M. Silver

RECEIVED
LAWRENCE
BERKELEY LABORATORY

AUG 28 1979

LIBRARY AND
DOCUMENTS SECTION

April 1978

TWO-WEEK LOAN COPY

This is a Library Circulating Copy which may be borrowed for two weeks. For a personal retention copy, call Tech. Info. Division, Ext. 6782

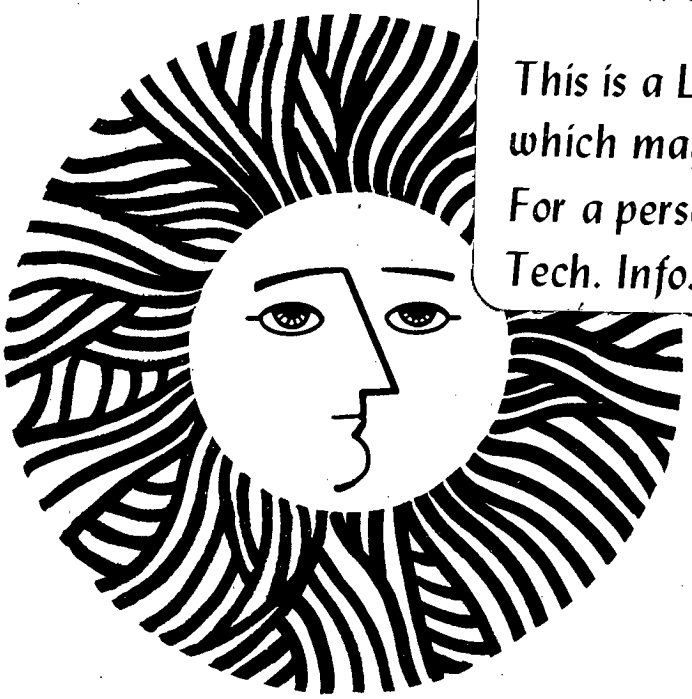

Prepared for the U. S. Department of Energy under Contract W-7405-ENG-48
and the Department of Navy, Naval Sea Systems Command,
under Contract N00017-72-C-4401

LBL-9539 c.2

DISCLAIMER

This document was prepared as an account of work sponsored by the United States Government. While this document is believed to contain correct information, neither the United States Government nor any agency thereof, nor the Regents of the University of California, nor any of their employees, makes any warranty, express or implied, or assumes any legal responsibility for the accuracy, completeness, or usefulness of any information, apparatus, product, or process disclosed, or represents that its use would not infringe privately owned rights. Reference herein to any specific commercial product, process, or service by its trade name, trademark, manufacturer, or otherwise, does not necessarily constitute or imply its endorsement, recommendation, or favoring by the United States Government or any agency thereof, or the Regents of the University of California. The views and opinions of authors expressed herein do not necessarily state or reflect those of the United States Government or any agency thereof or the Regents of the University of California.

Reactive and Inelastic Scattering of $H_2 + D_2$ Using a Repulsive Model Potential Energy Surface*

Nancy J. Brown
Department of Mechanical Engineering and
Energy and Environment Division, Lawrence Berkeley Laboratory
University of California
Berkeley, California 94720

and

David M. Silver
Applied Physics Laboratory
The Johns Hopkins University
Laurel, Maryland 20810

* This research was supported in part by Energy Research and Development Administration under Contract No. W-7405-ENG-48 at the Lawrence Berkeley Laboratory Energy and Environment Division, and in part by the Department of the Navy, Naval Sea Systems Command under Contract No. N00017-72-C-4401 at The Johns Hopkins University Applied Physics Laboratory.

ABSTRACT

Collisions between hydrogen and deuterium molecules are examined using quasiclassical dynamical trajectory calculations with the intermolecular field specified by a semi-empirical potential-energy surface incorporating enough repulsive character to yield barriers to chemical exchange that are in general agreement with ab initio results. The trajectory calculations are performed at high total system energies to permit the possibility of reactions. In addition to non-reactive inelastic collisions, the reactants H_2+D_2 can produce four possible reactive cases with product species $2H+D_2$, H_2+2D, HD+H+D and 2HD, respectively. The results are presented in terms of reaction probabilities, average final state properties of the molecules, and average final state energy distributions.

I. Introduction

A prototype for bi-molecular collision processes is the $H_2 + D_2$ system: $H_2 + D_2 \rightarrow 2\ HD$. Even here, the corresponding interaction potential must have a complicated form in order to describe all of the various intra-molecular and intermolecular effects that are present. The dominant contributions to the potential should arise from two-atom effects: that is, a sum of interactions obtained by considering each possible pair of atoms independently of the others. These effects should be adequately described by the London-type potentials that have been used in previous classical dynamics studies[1-6] of bimolecular collisions. However, especially at short intermolecular separations, important contributions to the potential can also arise from three-atom and four-atom effects: that is, a sum of terms derived from the simultaneous interactions of three and four atoms, respectively.

Previous quasi-classical dynamics studies of bimolecular collisions[1-6] have employed semi-empirical potential energy surfaces[7-14] that are restricted to the inclusion of two-atom effects, through use of the London approximation[7]. For $H_2 + D_2$, such model potential energy surfaces have saddle-point barriers to the chemical exchange process that are approximately one-half as high as the lowest barriers found from ab initio calculations.[15-22] Although two atom effects are dominant, three and four atom effects are important to the physical picture and their inclusion brings the model barrier heights in line with the ab initio barriers.

The present work reports details of quasi-classical trajectory calculations for collisions between H_2 and D_2 using a model potential energy surface having strong repulsive features. The surface employs a

valence bond model with semi-empirical evaluation of integrals, including many-atom contributions. In agreement with ab initio results, the energy barriers to chemical exchange on the model surface are all greater than the energy required to dissociate a single hydrogen molecule.

The total system energy employed in the trajectory calculations is maintained at levels above the H_2 dissociation to permit the possibility of chemical exchange. The results are presented in terms of reaction probabilities, average final state properties of the molecules, and average final state energy distributions. The influence of various initial vibrational and rotational energy distributions is examined. In particular, since the experimental observations of the $H_2 + D_2$ system have been shown to be consistent with vibrational excitation of at least one of the reactant molecules[23-29], several of these posibilities are examined in detail to study reactivity as a function of initial energy distribution.

The model potential surface is presented in Section II. A description of collision procedures is given in Section III. The results of the collision calculations are reported in Section IV for both reactive and inelastic non-reactive cases. A discussion of the results and their relationship to experimental observations follows in Section V.

II. Repulsive Model Potential Energy Surface

The potential function employed in the present work consists of the nuclear-nuclear repulsion energy plus a semi-empirical valence bond description[8-11,30] of the interactions between four electrons about four protons. Isotopic differentiation of the four nuclei is suppressed in this Section and the nuclei are labelled A, B, C and D.

The valence bond wavefunction for the four-electron, four-atom system[31] consists of two covalent structures: (i) an A-B bond and a C-D bond; (ii) an A-C bond and a B-D bond. The relative importance of these structures is determined by the variation principle. The atomic wavefunction on each center is a hydrogenic 1s atomic orbital. If all one-electron and two-electron integrals are explicitly evaluated, the result is an ab initio valence bond description of the H_4 system[15,18], which is a reasonable approximation to the corresponding "single-zeta" full configuration interaction procedure[32].

To obtain a tractable analytical form for the H_4 potential surface and its derivatives, a semi-empirical evaluation[11] of the various electronic integrals is necessary. A parameterization of the integrals has been chosen[30] that gives the proper atomic (4 H) and diatomic (2 H_2) asymptotic limits, each H_2 molecule being described by a Morse potential[33]. With one atom removed, the H_4 surface reduces to the Porter-Karplus[11] potential for three atoms (H_3). The remaining parameters governing the repulsive four-atom effects are chosen to give agreement with ab initio calculations of the H_4 potential.

Since the semi-empirical model H_4 surface is developed from a "single zeta" ab initio valence bond surface, a logically consistent procedure is to choose values for the repulsive four-atom parameters such that these two surfaces are in reasonable agreement. Table I gives a comparison between the ab initio valence bond and configuration interaction results and the semi-empirical "repulsive" potential for the minimum energy square-planar conformation of H_4. These results are all in reasonable agreement, especially in comparison with the corresponding result on a London potential, given in Table I.

A further comparison is presented in Figure 1, showing the interaction energy along a rectangular reaction path leading to a square intermediate. The ab initio and repulsive reaction paths cross a saddle-point at the intermediate position, $x = y = 2.7$ bohr, and thus the reaction path shown in Fig. 1 is close to a reaction path of steepest ascent. In contrast, the London path shown in Fig. 1 is far from its steepest ascent reaction path, since the saddle-point on the London surface occurs at $x = y = 1.94$ bohr with an interaction energy of ≈ 0.12 hartree. This is more evident from the equipotential contour maps in Fig. 2 corresponding to the rectangle-square-rectangle surfaces.

The most striking difference between the London and repulsive potentials is the height of the saddle-point barrier in the square geometry, $x = y$ in Fig. 2. Further differences also appear in the shapes of the reactant and product valleys, as can be seen in the projected views of the rectangular contour maps given in Fig. 3. A comparison of energy minima and their positions in other symmetric intermediate geometries is presented in Table II for the repulsive and London potentials.

III. Description of the Collision Procedure

A. Trajectory Calculations

The methods of quasiclassical collision dynamics are used to study the $H_2 + D_2$ collisions on the repulsive model potential energy surface. The conjugate co-ordinates and momenta, the reduced masses, the co-ordinate system and the boundary conditions are defined in our previous study.[6] The numerical procedures, namely the use of a fourth-order Runga-Kutta algorithm to solve the equations of motion and the use of a composite generator for random number generation, have also been previously described.[6] Atomic units[6] are used throughout these calculations.

A set of trajectories is defined to consist of 300 trajectories, each trajectory having an initial energy configuration identical to the other trajectories in the same set, but different values of Monte Carlo variables governing the initial orientation and phases of the reactants. To fascilitate comparison between the various sets and to produce a degree of uniformity in the convergence of the Monte Carlo averaging process from one set to the next, the same collection of Monte Carlo variables is used for each of the various sets. Hence, the random numbers used for the nth trajectory of one set is used for the nth trajectory of all other sets.

A given set of trajectories is characterized by a quadruple of numbers, the initial H_2 rotational quantum number, the initial H_2 vibrational quantum number, the initial D_2 rotational quantum number and the initial D_2 vibrational quantum number, and the notation $(j_{H_2}\ v_{H_2}\ j_{D_2}\ v_{D_2})$ is used to identify each particular set. In this study, initial rotational quantum numbers are chosen to be zero or three.

The total system energy for most trajectory sets is .24 hartree; however, the initial distributions of energy between relative translational, rotational and vibrational energy of the molecules are varied. This high system energy insures a reasonable level of reactivity so that statistically meaningful Monte Carlo averages can be obtained for reaction probabilities with relatively few trajectories.

Preliminary calculations revealed that the impact parameter cut-off for reactivity is 1.0 bohr. Since most reactions occur at small impact parameters and one of the objectives of this investigation is to study reactivity as a function of initial energy configuration, a constant initial impact parameter of 0.1 bohr was selected for all the trajectories computed. The choice of a constant impact parameter has the additional advantage that the statistical variation among various sets of trajectories is reduced for a given number of trajectories. The consequence of this choice is, however, that one cannot then compute reaction cross sections which are a prime ingredient of rate coefficients. However, in the case of molecule-molecule collisions, restriction to reaction probabilities is not a severe liability since the calculation of a rate coefficient is a formidable task due to the multiplicity of variables which must be averaged to span the phase space.

B. Final Conditions

Since a trajectory can lead to a chemical reaction, a simple distance criterion is not available as a means of terminating the trajectory. Instead, each trajectory is integrated for a time, t = 800 a.t.u., the two

smallest inter-particle distances, r_m and r_n, are identified, and the potential energy of the system, V_s, is evaluated. The trajectory is terminated when

$$\text{Morse } (r_m) + \text{Morse } (r_n) + 5 \times 10^{-4} > V_s$$

since this implies that the molecules are no longer interacting. This criterion has been checked for several trajectories and found satisfactory.

Five different types of reaction are possible outcomes of a given trajectory:

$H_2 + D_2 \rightarrow H_2 + D_2$ (non-reactive--Case I)

$H_2 + D_2 \rightarrow 2H + D_2$ (H_2 dissociation--Case II)

$H_2 + D_2 \rightarrow H_2 + 2D$ (D_2 dissociation--Case III)

$H_2 + D_2 \rightarrow HD + H + D$ (single exchange--Case IV)

$H_2 + D_2 \rightarrow 2HD$ (double-exchange--Case V)

The procedure for determining which of these reactions has occurred involves the identification of the product species. When the trajectory is terminated, the labelling of the two smallest inter-particle distances, r_m and r_n, is examined. Since the reactant molecules are taken to be AB and CD, then if m and n correspond to AB and CD, Case I obtains and reaction has not occurred. If m and n correspond to another combination of labels, a check is made to determine whether r_m or r_n is greater than or equal to 5.6 bohr. If so, Cases II, III or IV are possible outcomes, and the specific case is identified by determining the smaller distance. If m and n are

either AC and BD or AD and BC with both of the corresponding distances smaller than 5.6 bohr, Case V occurs.

After the particular reaction path is identified, it is of interest to study the characteristics of the energy transfer occurring in both the reactive and non-reactive collisions. If reaction paths I or V occur, the previously described procedure[6] for each is followed to determine the final rotational ($\bar{E}_j$) and vibrational ($\bar{E}_v$) energies of the two molecules and the relative kinetic ($\bar{E}_k$) energy. If reaction paths II or III occur, these are treated in a manner similar to path I.[6] If reaction path IV obtains, a coordinate transformation is made, the final relative kinetic energy is computed from the appropriate conjugate momenta and the final rotational and vibrational energy of the single molecule is computed.[6]

Final rotational and vibrational states for each molecule are determined and designated by the rotational and vibrational quantum numbers, j' and v', respectively. A scattering angle χ and the maximum value of the potential energy along each trajectory, referred to as the barrier, B, are also determined. For a given set of trajectories, the averages of the rotational, vibrational and kinetic energies are computed and designated by $\langle \bar{E}_j \rangle$, $\langle \bar{E}_v \rangle$ and $\langle \bar{E}_k \rangle$ respectively. The average barrier $\langle B \rangle$ and average scattering angle $\langle \chi \rangle$ and distribution of the final rotational and vibrational states are also determined for each trajectory set. The procedures for calculating the above quantities have been described.[6]

IV. RESULTS

In this section, the reactivity and energy transfer of fifteen sets of trajectories are discussed. Eleven sets have a total energy of 240 millihartree but differ from one another in their distribution of energy into rotational, vibrational and translational degrees of freedom. Each of the remaining four sets has an internal energy identical to one of the previous sets but has a different total energy. The fifteen sets are selected to investigate the effects of initial energy distribution on the total and specific reactivity and energy transfer.

Table III provides a summary of results for the various trajectory sets. The initial energy distribution according to kinetic energy, rotational energy of each molecule, vibrational energy of each molecule and the percent reactivity for each reaction path are listed in the table. In general, the trajectories are highly unreactive (case I): seven of the fifteen sets are greater than 90% unreactive and the remaining eight are between 65 and 90% unreactive. The next most likely outcome of a trajectory is H_2 dissociation (case II).

A. Non-Reactive Trajectories

A summary of the characteristics of the non-reactive trajectories is given in Table IV. For each trajectory, we define the barrier B to be the maximum potential energy along the trajectory. It is interesting to note that the average barrier, $\langle B \rangle$, for each set of trajectories is approximately 87 percent of the total energy of that set.

A second characteristic of the non-reactive trajectories is that they have a nearly constant value of average scattering angle, $\langle \chi \rangle$. The average values for the various sets have a standard deviation that is no more than 7 degrees and usually less than 3 degrees. The small deviations

indicate that the scattering angle is strongly influenced by the central force portion of the potential. Since the initial impact parameter is the same for each of these trajectories, the near constancy of the average scattering angles for the various sets, irrespective of the initial energy conditions, reflects the strong repulsive nature of the potential and the tendency for the collisions to resemble hard sphere interactions. The scattering angle for this limiting case of hard spheres in determined from the expression

$$\chi = 2 \arccos (b/d)$$

where b is the impact parameter and d is the distance between centers and is equivalent to the "molecular diameter". Taking b = 0.1 bohr and values for d of $\frac{1}{2} r_e$ to 2 r_e, the variation in scattering angle is 164° to 176°. Although this range brackets the values of $<\chi>$ in Table IV, the trajectories are apparently more complicated than hard-sphere trajectories as evidenced by the variation in the redistribution of energy in the final states.

To examine the effect of initial kinetic energy with the remaining internal energies held constant, sets with the same indices but different total energy are compared: e.g., compare the two (0000) sets having total energy 240 and 330 millihartree, respectively. The average kinetic energy loss increases monotonically with increased initial kinetic energy. The average final rotational energy change of each molecule also increases with initial kinetic energy, which probably reflects the increased angular momentum of the sets with higher initial kinetic energy. The distribution of final rotational states is only slightly influenced by the initial kinetic energy, as shown in Fig. 4 for the (0303) case.

The distribution of final vibrational states for this case is also given in Fig. 4. The collisions become more inelastic with respect to vibrational energy change with increasing kinetic energy and there is a tendency for the distribution of final vibrational states to broaden. Since the average vibrational energy changes, $\langle \Delta E_v \rangle$ given in Table IV, include both excitations and de-excitations, the possibility of a systematic dependence on initial kinetic energy is somewhat masked. Nevertheless for D_2, a direct correlation can be seen between $\langle \Delta E_v \rangle$ and initial E_k.

Increased initial rotational energy has little effect on the energy transfer process. This is determined by comparing sets that differ only in initial rotational energy: (0000) with (3030); (0303) with (3333); and (0204) with (3234). The final rotational state distribution is peaked about the initial j value for both molecules and the number of final j states exhibits little dependency on the initial rotational energy. The vibrational state distributions are similarly unaffected by changes in initial rotational energy of this magnitude.

The effect of adding initial vibrational quanta to <u>both</u> molecules in incremental amounts for sets of the same total energy is examined by comparing the sets (0000), (0101), (0202), and (0303) in Table IV. Since the total energy is the same for each of these sets, the increased vibrational energy is obtained at the expense of relative translational energy. The final average kinetic energy loss decreases with increased vibrational excitation, which is consistent with the direct dependence of $\langle \Delta E_k \rangle$ on initial E_k noted above. The final rotational state distributions show little variation in this series and reflect the slight changes noted in the final average rotational energy. The average vibrational energy change of both molecules decreases with increased initial quanta. This cannot be attributed to decreased initial kinetic energy since this effect does not occur for both

molecules in the sets where kinetic energy is the sole variable. The final vibrational state distributions for the two molecules behave similarly to one another. For sets where transitions $\Delta v = \pm i$ are possible, i.e., other than (0000), the de-excitation is more probable than the corresponding excitation and accounts for the decreased average final vibrational energy of this series. With the exception of (0000), the total number of populated states shows little variation with the increased initial quanta.

The sets (0008), (0204), (0303) and (0500) are examined to ascertain the effect of initial vibrational energy distribution between the two molecules. These sets have the same total energy, nearly the same initial kinetic and total vibrational energy, but the vibrational energy is distributed differently between the molecules. The rotational energy gain of H_2 in the (0500) set and for D_2 in the (0008) set are the largest entries in their respective columns, and may indicate intramolecular energy transfer. The vibrational energy gain is higher for the molecule with the lesser amount of initial vibrational energy and the effect is more exaggerated when one of the molecules has the greater bulk of initial vibrational energy. The H_2 in (0500) and the D_2 in (0008) lose vibrational energy, which appears to account for most or all of the relatively large gains of the other molecule.

Finally, the effect of increasing the vibrational energy in <u>one</u> molecule at the expense of initial translational energy is estimated through comparison of (0000) with (0008), (0202) with (0204), (0300) with (0303) and (0000) with (0300) and (0500). As the initial vibrational energy of one of the molecules increases, the final average kinetic energy loss decreases; however, this trend is also present when initial kinetic energy is the sole variable. The final average rotational energy increases for the molecule with increasing initial vibrational energy, while the final average rota-

tational energy of the other molecule decreases. Also, the final rotational state distribution of the molecule whose initial vibrational state is altered has higher rotational states populated as the initial vibrational energy increases, and the other molecule has fewer final rotational states populated. The average vibrational energy change of both molecules decreases as the initial vibrational energy of one of them increases. This effect cannot be attributed entirely to the initial kinetic energy decrease since this effect did not occur for both molecules when kinetic energy was the sole variable. As the initial vibrational energy of a molecule increases, the maximum vibrational state populated for that molecule increases. No pattern emerged for the molecule with constant initial vibrational energy.

In summary, the results of the non-reactive trajectory calculations indicate the following trends. The energy transfer process is dominated by $T \rightarrow V$ and $T \rightarrow R$. Increasing initial kinetic energy increases the energy transfer from translational to internal modes. Initial rotational excitation shows no strong effects on the collision processes. There is some evidence for energy transfer between the internal modes. For example, as the initial vibrational energy of one of the molecules is increased, it acquires more rotational energy and loses vibrational energy while the other molecule gains less rotational energy.

B. Reactive Collisions

Average barriers $\langle B \rangle$ and scattering angles $\langle \chi \rangle$ are reported for the various sets of trajectories for each of the four reaction cases in

Tables V-VIII, respectively. In addition, the Tables present average final energy distributions of the reactive trajectories. These results provide the basis for most of the discussion presented below. However, histograms of final rotational and vibrational state distributions for the various cases have been constructed, and will also be discussed.

For each set of trajectories in Table V having more than 5% H_2 dissociation, the average barrier is 5-10% lower than the barrier for the corresponding unreactive case in Table IV. However, the scattering angle for a given set is only slightly less for the H_2 dissociation case than the corresponding non-reactive case. A similar pattern holds for the one set (0008) giving a significant D_2 dissociation in Table VI. The average deviations about the average scattering angle for these two dissociation reaction cases is relatively small (less than $\pm$ 13°). This preferential scattering and the close proximity of the $\langle\chi\rangle$ values to the unreactive case provide some evidence for the direct nature of these reactive collisions as opposed to the idea that an intermediate complex is formed during the course of the collision. In a direct reactive collision, the reaction is over before the colliding reactants have time to undergo rotations about one another. If the reactants form a complex which sticks together for a rotational period or more, the products fly off at random, giving an isotropic distribution of scattering angles.

The average scattering angles of about 90° observed for the single and double exchange reactions in Tables VII and VIII differ significantly from the average non-reactive $\langle \chi \rangle$ value of $\sim$172°. Moreover, the average deviations for the single exchange case are as large as $\pm$ 28°. Thus, trajectories leading to chemical exchange correspond to a collision mechanism that is quite distinct from the more direct mechanism that appears to control the non-reactive and dissociation collision cases.

The effect of initial kinetic energy variation can be examined by comparing sets with the same indices and different total energy; that is, the two (0204) sets and the three (0303) sets. Total reactivity increases with increasing initial kinetic energy, especially the specific reactions, H_2 dissociation and single exchange. As the initial kinetic energy increases, the energy used for dissociation appears to come preferentially from kinetic energy, since the final kinetic energy loss increases and final vibrational loss decreases. The double exchange process is slightly more probable as kinetic energy is increased although the slight increase may not be statistically significant. The total internal energy of the product HD formed in both exchange reactions increases with increasing initial kinetic energy. The increase in HD rotational energy reflects the increased total angular momentum of the system, with increased kinetic energy.

The effect of initial rotational energy on reactivity is determined by comparing sets that differ only in initial rotational energy: (0303) with (3333); and (0204) with (3234). Initial rotational energy changes of this magnitude are seen to affect no significant change in reactivity. Single exchange decreases with increasing initial rotational energy in comparing (0303) with (3333). Increasing initial rotational energy could act to decrease the probability of geometrically favorable orientations which lead to reaction.

The effect of holding the total energy constant and adding vibrational quanta of energy in incremental amounts to <u>both</u> reactant molecules at the expense of initial kinetic energy is determined by comparing the (0000), (0101), (0202) and (0303) sets. From Table III, the total reactivity

increases with the addition of successive quanta and there is an increasing number of reaction cases having probabilities greater than zero. For H_2 dissociation, the reactivity for (0101) is very low, whereas for the (0202) and (0303) sets it is $\sim$5%. Since the latter two sets differ from one another only in a transfer of $\sim$30 millihartree from initial kinetic to initial vibrational energy, these two initial energy modes are seen to be equally effective in producing H_2 dissociation within this series. For single exchange, the initial vibrational energy is more effective than initial kinetic energy since the reactivity increases from 2 to 7% between the (0202) and (0303) sets. In Table V, the ratio of final kinetic energy loss to initial kinetic energy is approximately constant for this series. As vibrational quanta are added to the two molecules, the vibrational energy of D_2 seems to increasingly contribute to the dissociation of H_2. For the single exchange process in Table VII, the internal energy of the product HD decreases with added initial vibrational quanta.

Next, the sets (0008), (0204), (0303), and (0500) which have the same total energy, nearly constant initial kinetic energy but various distributions of initial vibrational energy are examined. There are significant differences in overall and specific reactivity which implies that it is the distribution of vibrational energy between the reactant molecules that is of more consequence to reactivity than the total amount. This is in marked contrast to atom-molecule scattering. Placing most of the initial vibrational energy in one of the reactants produces the dissociation of that reactant as evidenced by the relatively large number of H_2 dissociations in the (0500) set and correspondingly large number of D_2 dissociations in the (0008) set. H_2 dissociates more easily than D_2 for a given amount of initial vibrational energy. If one considers dissociation as an extreme case of vibrational energy transfer, this effect can be explained

by the greater ability of H_2 to acquire vibrational energy than D_2. This will be discussed in more detail subsequently. Distributing the vibrational energy more equally between the molecules increases the occurence of single exchange reactions. The (0204) and (0303) sets are nearly equivalent energetically: however, in the former case, D_2 has the greater share of initial vibrational energy while in the latter, the converse obtains. In comparing the two sets, the (0303) set has a larger number of H_2 dissociations while the number of single exchange reactions is only slightly greater for the (0303) set. Also, the final average HD vibrational energy in single exchange is similar for the two sets. The same trends are seen when the (0204) and (0303) sets of total energy $\sim$270 millihartree are compared.

The effect of changing the vibrational energy for <u>one</u> molecule at the expense of initial kinetic energy can be examined as follows. Comparing sets (0000) with (0008) or (0000) with (0300) and (0500), an increase in the initial vibrational energy of one of the molecules while the other remains initially in $v = 0$ produces an increased number of dissociations of the excited molecule. Comparing sets (0202) with (0204) or (0300) with (0300), the increase in initial vibrational energy of one of the molecules while the other molecule remains initially in $v > 0$ enhances the probability for exchange reactions but decreases the probability for dissociation.

H_2 dissociation occurs largely through kinetic energy transfer with an average barrier greater than the dissociation energy, 174 millihartree. As the vibrational energy of D_2 increases, more of the vibrational energy is used for H_2 dissociation. Little rotational energy is transferred to D_2 and the final rotational states populated are $j'_{D_2} \leq 6$. The initial rotational state of D_2 is also the most populated final state. The change from initial to final vibrational quantum number of D_2 is no greater than

$\Delta v = \pm 3$, with the probability of de-excitation increasing with increasing initial v_{D_2}.

The D_2 molecule is more difficult to dissociate than H_2. The difference in mass of the two molecules is responsible for the relative ease with which H_2 gains vibrational energy and dissociates relative to D_2. If one examines the vibrational energy transfer in the spectator limit of atom-molecule collisons, i.e. letting D_2 be a particle in one case and H_2 be a particle in the reverse, the lighter mass molecule colliding with the heavier mass particle gains vibrational energy more easily than the reverse situation of a heavier molecule colliding with a light mass particle. This is shown simply by momentum conservation for a linear collision.[34] Physically, this implies that the duration of the collision is short compared to the period of the oscillation. The scattering angles associated with both dissociation reactions reflect that the atoms of the dissociated molecule are back scattered from the remaining molecule.

Details of the single exchange process are given in Table VII. The single exchange reaction appears more probable for those sets which have the initial vibrational quantum number of each molecule greater than or equal to two. Comparing the two (0204) sets and the three (0303) sets indicates that increased initial kinetic energy enhances the probability of single exchange. The deviations from the average scattering angle of approximately 90 degrees are larger than those associated with the other reactive paths. The product HD has a final rotational quantum number $j'_{HD} \leq 11$ with an even distribution over the final states. In general, the final average rotational energy of HD is higher than that present in the undissociated molecule in the collisionally induced dissociation reactions. The

final vibrational states of HD are such that $v'_{HD} \leq 3$ with the states $v' = 0$, 1 being most heavily populated. The relative kinetic energy of the unbonded H and D atoms is less than but of the same order of magnitude as the final relative kinetic energy.

Unfortunately the probability for the occurrence of a double exchange reaction is very low and therefore only a small number of trajectories follow this path. Nevertheless, a few observations of the results in Table VIII are of interest. For each set of trajectories where double exchange occurs, a larger number of single exchanges occur and the average barriers for double exchange are higher than the corresponding average barriers for single exchange. The average scattering angles of $\sim 90^{\circ}$ are quite similar in the single and double exchange cases; however, the deviations from the average values of χ for double exchange are smaller than those in the single exchange process. With one exception, the trajectories which lead to double exchange all involve an H_2 with an initially expanding bond (positive vibrational phase) and a D_2 with an initially contracting bond (negative vibrational phase). For some sets, there is a significant rotational excitation of the HD molecules, with population of rotational states up to $j' = 14$. In all but one trajectory, one of the HD molecules is vibrationally excited to $v'_{HD} \geq 8$ while the other HD molecule is in a low vibrational state.

V. Discussion

Collisions between H_2 and D_2 would traditionally be expected to give rise to some H_2 dissociation (Case II), D_2 dissociation (Case III), and double exchange (Case V). Thus, it is interesting to observe the occurrence of the single exchange reaction (Case IV). It appears that the four-center single exchange reaction has its own collection of reaction paths that are energetically intermediate between dissociation and double exchange. For example, (i) lower average barriers are observed and less initial vibrational energy is required for single exchange than double exchange; (ii) the reactive paths for single exchange have higher average barriers and appear to require higher vibrational energy thresholds than the dissociative paths. The trajectory times associated with single exchange collisions are one and a half to two times longer than other reactive trajectories but are considerably less than times one might associate with rotational periods of four-center complexes. Moreover, there is no other evidence for a long lived collision complex along the single exchange reaction path: the distribution of scattering angles is not isotropic between 0 and π even though large standard deviations are associated with the average scattering angles of the single exchange case. Finally, the rather stringent requirement of reactant molecules having vibrational phase of opposite signs which was noted for double exchange reactions is absent for the single exchange case.

Although it would be of interest to compare collisions on the valence bond repulsive surface with the previously described[1] collisions on the London surface, the comparison is not parallel since the London surface has a lowest energy saddle point barrier to chemical exchange of

0.116 hartree, collisions were studied at energies greater than the barrier height and less than the H_2 dissociation energy. Thus the number of possible reaction paths were restricted to the non-reactive and double exchange cases.

In the London study, reactivity decreases with initial vibrational energy, while here, the probability for double exchange is enhanced by increased vibrational energy in both molecules. The final internal energy distribution of the product HD molecules for both studies is different. Both HD molecules have $v' \leq 4$ in the London study; while here, one of the product HD molecules is highly excited with $v' \geq 8$, and the other is in a low vibrational state. The final rotational state distributions of the HD products are somewhat different; $j' \leq 10$ obtains for London double exchange while $j' \leq 14$ is found here.

There are more similarities for non-reactive collisions than for reactive collisions on both surfaces. The scattering angles associated with the nonreactive collisions on both surfaces are principally determined by the central force portion of the interaction. Here, due to the strong repulsive nature of the surface, the scattering angle is approximately independent of the initial energy distribution, while calculations on the London surface with its softer repulsive wall yield average scattering angles which are inversely related to initial kinetic energy. The major mode of energy transfer for both studies appears to be the transfer of kinetic energy into the internal degrees of freedom. Average kinetic energy changes are negative for the sets investigated in both studies; however, in the London study, $|\langle \Delta E_k \rangle|$ is monotonic with initial kinetic energy.

There are interesting effects which occur in both studies which emphasize the bimolecular nature of the collisions. With only two exceptions, the molecule with the greater initial vibrational energy has, on the average, the greater final rotational energy. The apparent intermolecular vibrational rotational coupling is emphasized by the following trend noted in collisions on both surfaces: $\langle \Delta E_j(H_2) \rangle$ decreases with $E_v(D_2)$ for constant $E_v(H_2)$ and equivalent behavior is noted with respect to the $\langle \Delta E_j(D_2) \rangle$ dependence on $E_v(H_2)$ for constant $E_v(D_2)$.

The $H_2 + D_2$ exchange reaction has been studied experimentally by several investigators[23,24,28,29] but the mechanism is not understood. Large discrepancies exist between experimentally derived activation energies and theoretical calculations [15-22] of barrier heights. Experimental results are, however, in agreement with one another with respect to an activation energy of 40 kcal/mole. If one assumes a quadratic time dependence, unit order dependence for the inert gas, and zero order dependence for H_2 and D_2, the experimental data all yield approximately the same value of the frequency factor. The rate law derived from experimental data has a unit order dependence on inert gas concentration, and this argues against a direct four-center mechanism. A dissociation reaction followed by an atom/molecule exchange step mechanism has a quadratic time dependence; however, this mechanism also requires a unit order dependence of the reactants and an activation energy of ~110 kcal/mole, which is considerably larger than the experimentally determined activation energy of 40 kcal/mole. Thus, this mechanism is inconsistent with the experimentally determined rate law. A vibrational excitation mechanism, in which only vibrationally excited molecules react via double exchange, is eliminated as a potential mechanism

if one includes vibrational de-excitation kinetics, since it does not reproduce the experimentally determined quadratic time dependence. This mechanism also requires a unit order dependence on reactants and is thus inconsistent with experimental results.

A stimulated raman laser study of the $H_2 + D_2$ exchange reaction has been reported[24] in which either H_2 or D_2 is excited to $v = 1$ in the presence of the other molecule. Modeling calculations[24] which included intramolecular and intermolecular vibrational energy transfer and chemical reaction were performed to describe the time evolution of the system and ultimate reactivity. These were in qualitative agreement with experimentally determined HD production levels, and it was thus concluded that exchange occurs with reasonable probability for collisions in which $v_{H_2} \geq 3$ or $v_{D_2} \geq 4$, and that translational energy was relatively unimportant in causing reaction.

The present study has been directed toward investigating some features of the bimolecular reaction. However, since reaction probabilities and not a rate coefficient are determined here, the results are not directly comparable with experiments in which a rate coefficient is determined. In addition, since the barrier to chemical exchange on the potential energy surface is very high, the trajectory calculations needed to be performed at high total energies in order to permit the possibility of reaction. Even at high total energy, less than 3% of the trajectories led to double exchange reactions, and therefore the statistical significance of these reaction probabilities is such that the results can only be viewed qualitatively.

Despite these difficulties and differences between the present calculations and the experiments, there are some interesting comparisons. Here, reaction via double exchange requires that both molecules are vibrationally excited and, in the collection of sets investigated, double exchanges occur only when $v_{H_2} = 2$ or 3 and $v_{D_2} = 3$ or 4. In particular, vibrational excitation is required in both molecules, in contrast to the mechanism of Bauer et al.[29] in which only one of the molecules needs to be vibrationally excited. Moreover, in the present work, dissociation and single exchange reactions are more probable than double exchange. Also, kinetic energy enhances the reaction probability for exchange once sufficient initial vibrational energy is present. The HD exchange products are vibrationally excited in agreement with the conclusions of Bauer et al.;[29] however, the amount of excitation differs due to the high kinetic energies considered here. The calculations of Bauer et al.[29] indicate that V-V energy transfer is of extreme importance in populating the upper, reactive vibrational states of the reactants. Here, due to the large initial translational energies, T-V transfer is by far the dominant process.

References

1. K. Morokuma, L. Pedersen and M. Karplus, J. Am. Chem. Soc. 89, 5064 (1967).
2. B. Shizgal and M. Karplus, J. Chem. Phys. 52, 4262 (1970).
3. B. Shizgal, J. Chem. Phys. 57, 3915 (1972).
4. L. M. Raff, D. L. Thompson, L. B. Sims and R. N. Porter, J. Chem. Phys. 56, 5998 (1972).
5. D. L. Thompson and D. R. McLaughlin, J. Chem. Phys. 62, 4284 (1975).
6. N. J. Brown and D. M. Silver, J. Chem. Phys. 65, 311 (1976).
7. F. London, Z. Elektrochem. 35, 552 (1929).
8. H. Eyring and M. Polanyi, Z. Phys. Chem. Abt. B 12, 279 (1931).
9. S. Glasstone, K. J. Laidler, and H. Eyring, "The Theory of Rate Processes", (McGraw Hill, New York, 1941).
10. S. Sato, J. Chem. Phys. 23, 592 (1955); Bull. Chem. Soc. Jpn. 28, 450 (1955).
11. R. N. Porter and M. Karplus, J. Chem. Phys. 40, 1105 (1964).
12. J. K. Cashion and D. R. Herschbach, J. Chem. Phys. 40, 2358 (1964).
13. L. M. Raff, L. Stivers, R. N. Porter, D. L. Thompson and L. B. Sims, J. Chem. Phys. 52, 3449 (1970).
14. R. B. Abrams, J. C. Patel and F. O. Ellison, J. Chem. Phys. 49, 450 (1968).
15. V. Magnasco and G. F. Musso, J. Chem. Phys. 46, 4015 (1967); 47, 1723 (1967); 48, 2834 (1968).
16. M. Rubinstein and I. Shavitt, J. Chem. Phys. 51, 2014 (1969).
17. O. Tapia, G. Bessis and S. Bratož, C. R. Acad. Sci. Paris 268B, 813 (1969); Int. J. Quantum Chem. S4, 289 (1971).
18. C. W. Wilson, Jr. and W. A. Goddard III, J. Chem. Phys. 51, 716 (1969); 56, 5913 (1972).

19. O. Tapia and G. Bessis, Theoret. Chim. Acta 25, 130 (1972).

20. C. F. Bender and H. F. Schaefer III, J. Chem. Phys. 57, 217 (1972).

21. E. Kochanski, B. Roos, P. Siegbahn and M. H. Wood, Theoret. Chim. Acta 32, 151 (1973).

22. D. M. Silver and R. M. Stevens, J. Chem. Phys. 59, 3378 (1973).

23. S. H. Bauer and E. Ossa, J. Chem. Phys. 45, 434 (1966).

24. A. Burcat and A. Lifshitz, J. Chem. Phys. 47, 3079 (1967).

25. D. Lewis and S. H. Bauer, J. Am. Chem. Soc. 90, 5390 (1968).

26. S. H. Bauer and E. L. Resler, Jr., Science 146, 1045 (1964).

27. S. H. Bauer, D. Marshall, and T. Baer, J. Am. Chem. Soc. 87, 5514 (1965).

28. R. D. Kern and G. G. Nika, J. Phys. Chem. 75, 1615, 2541 (1971).

29. S. H. Bauer, D. M. Lederman, E. L. Resler, Jr. and E. R. Fisher, Int. J. Chem. Kinetics 5, 93 (1973).

30. D. M. Silver and N. J. Brown, to be published.

31. J. C. Slater, Phys. Rev. 38, 1109 (1931).

32. L. M. Raff and R. N. Porter, J. Chem. Phys. 51, 4701 (1969).

33. P. M. Morse, Phys. Rev. 34, 57 (1929).

34. B. H. Mahan, J. Chem. Phys. 52, 5221 (1970).

Table I. Comparison of ab initio and semi-empirical results for minimum energy $^1B_{1g}$ square-planar H_4.

Surface	R_{min} (bohr)	$E_{min}(H_4)$ (hartree)	$E(2\ H_2)$ (hartree)	ΔE(barrier) (kcal/mole)
CI (ab initio)[a]	2.7	-2.0595	-2.2959	148
VB (ab initio)[b]	2.7	-2.0543	-2.2947	151
Repulsive	2.67	-2.1223	-2.3489	142
London	1.94	-2.2321	-2.3489	73

[a]Full configuration interaction, using a single-zeta basis set with optimized orbital exponents.

[b]Valence bond including all covalent structures, using the same basis set as for the CI calculation.

Table II. Singlet state energy minima for various geometrical conformations of H_4.

Geometry	Surface	R_{min} (bohr)	E_{min} (hartree)
Linear equidistant	Repulsive	1.80	-2.2710
	London	1.72	-2.2597
Centered equilateral triangle	Repulsive	2.31	-2.0767
	London	2.02	-2.0812
Tetrahedron	Repulsive	3.20	-2.0448
	London	2.25	-2.1172

Table III. Characteristics of trajectory calculations giving initial kinetic energy E_k, initial rotational energy E_j, initial vibrational energy E_v, and the percent reactivity of the various reaction cases.[a]

Set	Total Energy	E_k	$E_j(H_2)$	$E_j(D_2)$	$E_v(H_2)$	$E_v(D_2)$	% Un-reactive	% H_2 Dis-sociation	% D_2 Dis-sociation	% Single Exchange	% Double Exchange
(0000)	240	223	0	0	9.89	7.02	100				
(3030)	240	218	3.2	1.6	9.89	7.02	100				
(0101)	240	189	0	0	28.8	20.7	99.3	0.7			
(0300)	240	172	0	0	63.6	7.02	78.0	22.0			
(0202)	240	160	0	0	46.7	33.8	93.3	4.7		2.0	
(0500)	240	138	0	0	94.2	7.02	68.7	31.3			
(0204)	240	133	0	0	46.7	58.4	93.0	0.3	0.3	5.3	1.0
(3234)	240	130	2.9	1.3	46.7	58.4	94.7		0.3	4.0	1.0
(0008)	240	128	0	0	9.89	101.4	75.0		24.0	1.0	
(0303)	240	130	0	0	63.6	46.3	86.0	5.0		7.0	1.7
(3333)	240	125	2.7	1.5	63.6	46.3	87.0	5.7		4.3	2.3
(0000)	330	313	0	0	9.89	7.02	88.0	12.0			
(0204)	271	165	0	0	46.7	58.4	81.0	6.0	0.7	8.7	2.7
(0303)	270	160	0	0	63.6	46.3	73.3	15.0		9.3	1.7
(0303)	213	102	0	0	63.6	46.3	97.3			2.3	0.3

[a] Energy in milli-hartrees.

Table IV. Non-Reactive Trajectories (Case I)

Set	Total Energy	$E_k^{(i)}$	Number	$\langle B \rangle$	$\langle \chi \rangle$	$\langle \Delta E_k \rangle$	$\langle \Delta E_j(H_2) \rangle$	$\langle \Delta E_j(D_2) \rangle$	$\langle \Delta E_v(H_2) \rangle$	$\langle \Delta E_v(D_2) \rangle$
(0000)	240	223	300	214	173	-74.4	4.0	1.5	45.2	23.9
(3030)	240	218	300	211	174	-74.4	3.1	1.4	47.1	23.0
(0101)	240	189	298	209	173	-57.1	4.4	1.6	33.1	18.2
(0300)	240	172	234	215	172	-33.7	8.8	1.1	6.1	17.9
(0202)	240	160	244	210	172	-39.0	5.0	1.9	18.1	14.2
(0500)	240	138	206	213	171	-12.8	13.2	0.8	-15.2	14.2
(0204)	240	133	279	203	172	-26.4	3.3	2.2	14.1	7.0
(3234)	240	130	284	201	173	-26.0	2.3	2.5	15.8	5.7
(0008)	240	128	225	208	170	-13.8	1.7	7.9	19.1	-14.8
(0303)	240	130	258	207	172	-16.7	4.6	1.7	4.3	6.3
(3333)	240	125	261	205	172	-17.3	4.0	1.7	1.3	6.5
(0000)	330	313	265	293	172	-124.0	7.3	2.8	71.2	43.0
(0204)	271	165	244	231	171	-36.6	4.7	3.3	15.1	13.6
(0303)	270	160	220	233	171	-24.3	6.6	2.5	1.6	13.8
(0303)	213	102	292	187	173	-10.1	3.4	1.1	2.5	1.9

Energy in milli-hartrees.

Table V. H_2 Dissociation (Case II)

Set	Total Energy	$E_k^{(i)}$	Number	< B >	< χ >	$< \Delta E_k >$	$< \Delta E_j(D_2) >$	$< \Delta E_v(D_2) >$
(0101)	240	189	2	192	173	-130	—	-11
(0300)	240	172	66	195	168	-114	.3	4.7
(0202)	240	160	14	190	171	-107	.3	-17
(0500)	240	138	94	201	159	-83	.2	3.2
(0204)	240	133	1	216	148	-86	16	-57
(0303)	240	130	15	204	169	-89	.6	-20
(3333)	240	125	17	198	170	-85	.5	-22
(0000)	330	313	35	274	172	-173	1.3	9.9
(0204)	271	165	19	211	170	-100	.7	-26
(0303)	270	160	45	213	167	-98	1.1	-13

Energy in milli-hartrees

Table VI. D_2 Dissociation (Case III)

Set	Total Energy	$E_k^{(i)}$	Number	$< B >$	$< \chi >$	$< \Delta E_k >$	$< \Delta E_j(H_2) >$	$< \Delta E_v(H_2) >$
(0204)	240	133	1	197	144	-98	29	-42
(3234)	240	130	1	230	164	-102	-2.1	-9.7
(0008)	240	128	72	195	165	-74	.5	1.7
(0204)	271	165	2	218	152	-102	14	-24

Energy in milli-hartrees

Table VII. Single Exchange (Case IV)

Set	Total Energy	$E_k^{(i)}$	Number	$< B >$	$< \chi >$	$< \Delta E_k >$	$< E_j(HD) >$	$< E_v(HD) >$
(0202)	240	160	6	208	91.2	-125	5.9	25.9
(0204)	240	133	16	208	91.1	-87.6	5.1	13.9
(3234)	240	130	12	207	87.2	-82	5.2	12.4
(0008)	240	128	3	211	87.9	-71.6	1.8	8.1
(0303)	240	130	21	206	92.2	-79.8	2.9	13.4
(3333)	240	125	13	205	84.5	-78.1	6.0	12.4
(0204)	271	165	26	217	89.0	-95.8	6.1	21
(0303)	270	160	28	223	88.7	-93.6	7.5	22.8
(0303)	213	102	7	193	100	-72.7	2.1	7.4

Energy in milli-hartrees

Table VIII. Double Exchange (Case V)

Set	Total Energy	$E_k^{(i)}$	Number	$< B >$	$< \chi >$	$< \Delta E_k >$	$< E_j(HD) >$*	$< E_v(HD) >$*
(0204)	240	133	3	211	91.6	-81.0	2.5	90.7
(3234)	240	130	3	218	87.7	-66.4	8.3	79.7
(0303)	240	130	5	216	90.6	-85.7	9.3	88.6
(3333)	240	125	7	223	89.4	-79.8	14	83.1
(0204)	271	165	8	233	88.0	-94.1	13	86.7
(0303)	270	160	5	227	93.5	-89.4	8.4	91.3
(0303)	213	102	1	206	93.9	-81.4	4.3	91.4

Energy in milli-hartrees

* Average of both product molecules

Figure Captions

Fig. 1 Interaction energies along a reaction path corresponding to a rectangular arrangement of the two H_2 molecules, leading to a square-planar symmetric intermediate.

Fig. 2 Equipotential contour maps for the London and repulsive surfaces corresponding to rectangular arrangements of the four atoms. The contour intervals are one-tenth of the H_2 dissociation energy. The reaction paths in Fig. 1 are indicated here with dashed lines.

Fig. 3 Projection of the equipotential contour maps of Fig. 2 for the London and repulsive surfaces corresponding to rectangular arrangements of the four atoms. The contour intervals are one-tenth of the H_2 dissociation energy. The two surfaces are drawn to identical scale.

Fig. 4 Distribution of final rotational (j') and vibrational (v') states of H_2 and D_2 after nonreactive trajectories having the set of initial states (0303) and various values of initial kinetic energy E_k in hartree.

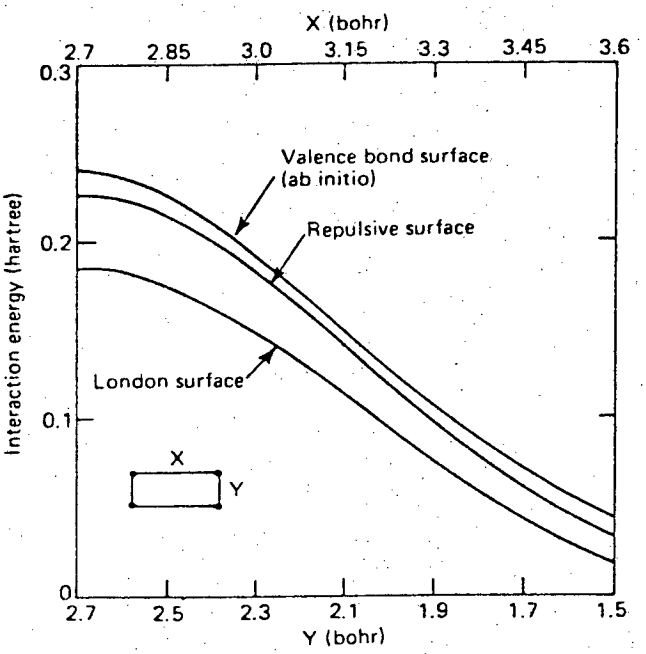
X (bohr)
2.7
2.85
3.0
3.15
3.3
3.45
3.6
0.3
0.2
0.1
0
Interaction energy (hartree)
Valence bond surface
(ab initio)
Repulsive surface
London surface
X
Y
2.7
2.5
2.3
2.1
1.9
1.7
1.5
Y (bohr)

FIGURE 1

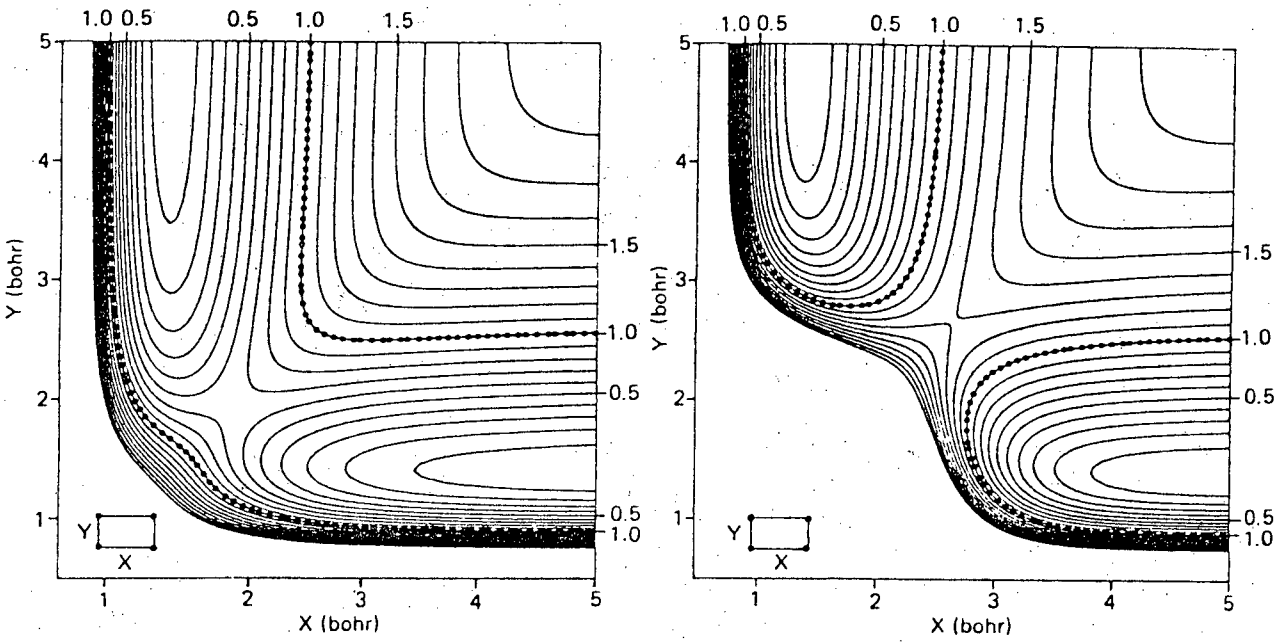

FIGURE 2

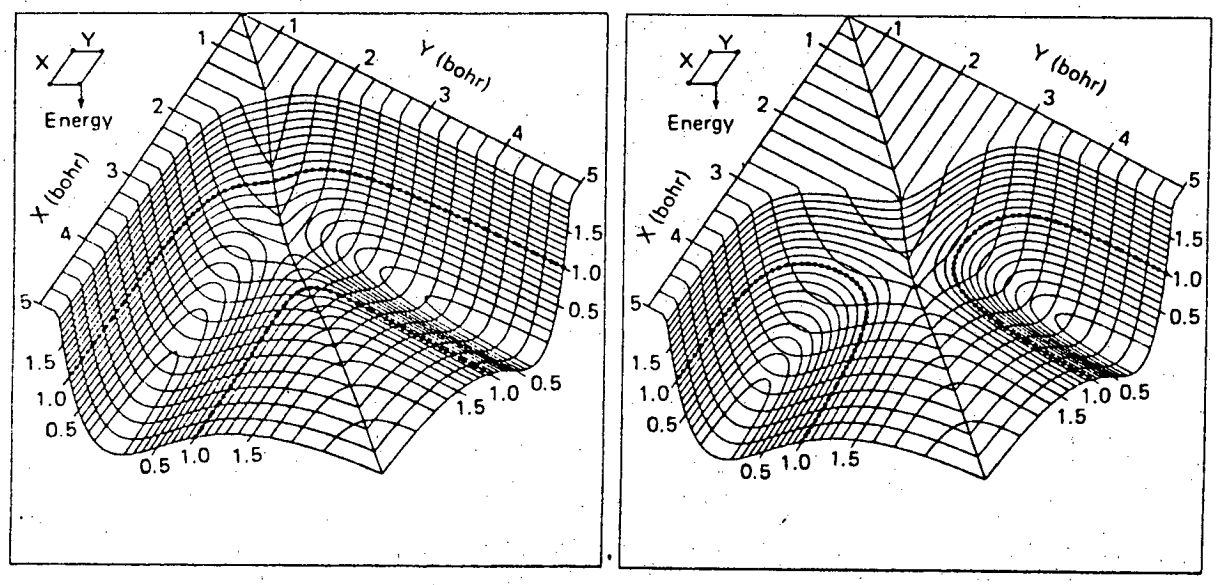

FIGURE 3

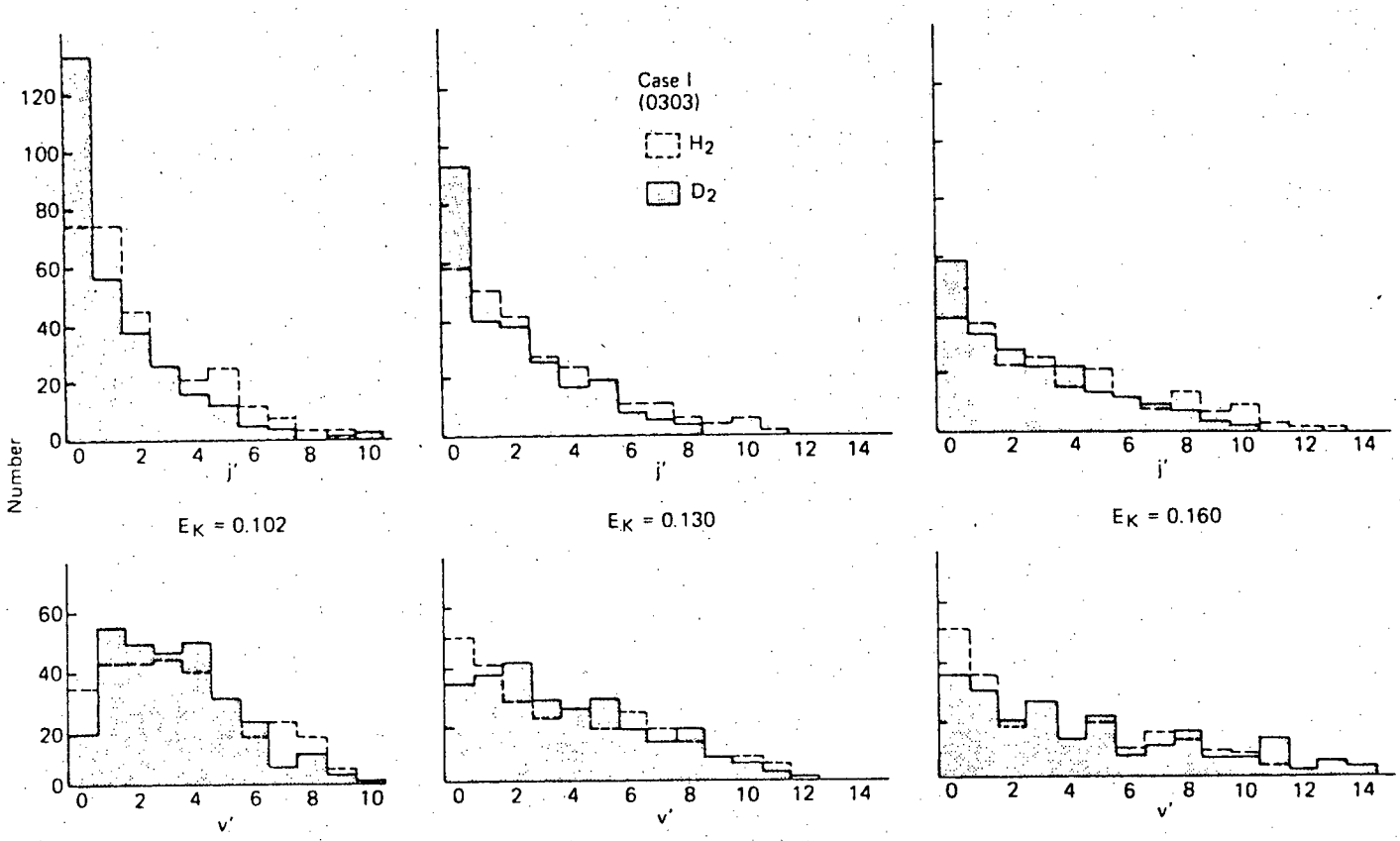

FIGURE 4

This report was done with support from the Department of Energy. Any conclusions or opinions expressed in this report represent solely those of the author(s) and not necessarily those of The Regents of the University of California, the Lawrence Berkeley Laboratory or the Department of Energy.

Reference to a company or product name does not imply approval or recommendation of the product by the University of California or the U.S. Department of Energy to the exclusion of others that may be suitable.

TECHNICAL INFORMATION DEPARTMENT
LAWRENCE BERKELEY LABORATORY
UNIVERSITY OF CALIFORNIA
BERKELEY, CALIFORNIA 94720